International Journal of Nanomedicine

Dovepress
open access to scientific and medical research

Open Access Full Text Article

ORIGINAL RESEARCH

Nanocalcium-deficient hydroxyapatite–poly (ε-caprolactone)–polyethylene glycol–poly (ε-caprolactone) composite scaffolds

This article was published in the following Dove Press journal:
International Journal of Nanomedicine
6 July 2012
Number of times this article has been viewed

Zhiwei Wang*
Ming Li*
Baoqing Yu
Liehu Cao
Qingsong Yang
Jiacan Su

Department of Orthopedics, Shanghai Hospital, Second Military Medical University, Shanghai, People's Republic of China

*These authors contributed equally to this work

Abstract: A bioactive composite of nano calcium-deficient apatite (n-CDAP) with an atom molar ratio of calcium to phosphate (Ca/P) of 1.50 and poly(ε-caprolactone)–poly(ethylene glycol)–poly(ε-caprolactone) (PCL–PEG–PCL) was synthesized, and a composite scaffold was fabricated. The composite scaffolds with 40 wt% n-CDAP contained well interconnected macropores around 400 μm, and exhibited a porosity of 75%. The weight-loss ratio of the n-CDAP/PCL–PEG–PCL was significantly greater than nano hydroxyapatite (n-HA, Ca/P = 1.67)/PCL–PEG–PCL composite scaffolds during soaking into phosphate-buffered saline (pH 7.4) for 70 days, indicating that n-CDAP-based composite had good degradability compared with n-HA. The viability ratio of MG-63 cells was significantly higher on n-CDAP than n-HA-based composite scaffolds at 3 and 5 days. In addition, the alkaline phosphatase activity of the MG-63 cells cultured on n-CDAP was higher than n-HA-based composite scaffolds at 7 days. Histological evaluation showed that the introduction of n-CDAP into PCL–PEG–PCL enhanced the efficiency of new bone formation when the composite scaffolds were implanted into rabbit bone defects. The results suggested that the n-CDAP-based composite exhibits good biocompatibility, biodegradation, and osteogenesis in vivo.

Keywords: nano calcium-deficient apatite, composite scaffold, degradability, cell responses, osteogenesis

Introduction

Studies have shown that nano hydroxyapatite (n-HA) has excellent biological performance, and was a potential candidate as a bioactive material for bone tissue repair.[1,2] Nevertheless, the extensive application of n-HA is still limited by its powder form and brittle nature. Biodegradable polymers and their copolymers are widely investigated and used in bone regeneration, dental repair, orthopedic fixation devices, as well as many other biomedical applications.[3–5] There currently exist no pure polymers that can effectively bond to bone tissue in vivo, and organic/inorganic bioactive composites of degradable polymers with bioactive inorganic phases are still a promising approach in developing bioactive biomaterials for bone regeneration.[6,7]

The copolymer, poly(ε-caprolactone)–polyethylene glycol–poly(ε-caprolactone) (PCL–PEG–PCL) has attracted much interest because of its cost-efficiency, degradability, toughness, and processibility.[8] PCL–PEG–PCL is a linear polyester copolymer composed of a hydrophobic poly(ε-caprolactone) (PCL) block and a hydrophilic polyethylene glycol (PEG) block; PCL and PEG are both well-known US Food and Drug Administration (FDA)-approved biomaterials and they are widely used in the biomedical field.[9] The PCL–PEG–PCL copolymer was prepared as drug-loaded nanoparticles or

Correspondence: Jiacan Su
Department of Orthopedics, Shanghai Hospital, Second Military Medical University, Shanghai 200433, People's Republic of China
Tel +86 21 8187 3400
Fax +86 21 8187 3398
Email jiacansu2012@yahoo.cn

thermosensitive hydrogel, and their physical–chemical properties and drug-delivery behaviors were investigated. The results reveal the good biodegradability and biocompatibility of PCL–PEG–PCL.[10] Previous studies have suggested that the variation in the atomic molar ratio of calcium to phosphate (Ca/P) greatly affected the solubility of the calcium phosphate biomaterials, and deficient calcium apatite with Ca/P ratio of 1.50 degraded faster than apatite with Ca/P ratio of 1.67 when implanted in vivo.[11,12] To obtain better bioperformance of apatite biomaterials such as higher bioactivity and faster degradation in vivo, nano-deficient calcium apatite (n-CDAP) with a Ca/P of 1.50 and its composite with PCL–PEG–PCL are fabricated in this study.

There have been a number of studies in the literature focusing on the biocomposites created by combining degradable polymers and nanoapatite.[13,14] However, there were few previous reports about the preparation of n-CDAP and PCL–PEG–PCL bioactive composite scaffolds for bone regeneration. It is expected that synthesis of n-CDAP with high degradability and bioactivity was used to compound with PCL–PEG–PCL; the degradability and bioactivity of the n-CDAP/PCL–PEG–PCL composite should be improved than in the n-HA/PCL–PEG–PCL composite scaffold. In addition, a combination of PCL–PEG–PCL with bioactive inorganic materials (n-CDAP) could enhance the advantages of both biomaterials. Therefore, in this study, n-CDAP/PCL–PEG–PCL composite scaffolds were prepared, and the primary cytocompatibility and osteogenesis of the composite scaffolds were investigated both in vitro and in vivo.

Materials and methods

Synthesis of n-CDAP

All the chemicals used in this study were purchased from Sinopharm Chemical Reagent Co, Ltd (Shanghai, China). The n-CDAP were synthesized using calcium nitrate ($Ca(NO_3)_2 \cdot 4H_2O$) and ammonium phosphate ($(NH_4)_2HPO_4$). First, calcium nitrate and ammonium phosphate (Ca/P mol ratio = 1.50) were dissolved separately in deionized water. The calcium nitrate solution was dropped very slowly into the ammonium phosphate solution while stirring at room temperature. The pH of the solution was kept between 10 and 12 by adding ammonium hydroxide. After the titration was finished, the mixture was set at room temperature for 24 hours. The resulting apatite precipitate was washed with deionized water five times, placed in a flask, and treated in water for 2 hours at 100°C. After treatment, the apatite precipitate consisted of n-CDAP in slurry (water). An aliquot was removed for transmission electron microscopy (FE-TEM; JEM-2100F; JEOL, Tokyo, Japan) testing. Furthermore, n-HA (Ca/P mol ratio = 1.67) was synthesized by using a similar method as a control.

Preparation of n-CDAP–PCL–PEG–PCL composite scaffolds

PCL–PEG–PCL with both hydrophobic PCL and hydrophilic PEG was synthesized as the raw material for fabricating composite scaffolds. A three-neck flask was purged with nitrogen and heated to 90°C. PEG methyl ether and a catalyst, stannous 2-ethylhexanoate, were introduced to the flask for 30 minutes. PCL was added to the flask to start the ring-opening polymerization at 120°C for 24 hours. In the purification process, the product was first dissolved in dichloromethane and then precipitated in a mixture of n-hexane and ethyl ether at a volumetric ratio of 3:7. This step was performed several times to purify the PCL–PEG–PCL product.

The n-CDAP–PCL–PEG–PCL composite scaffolds were prepared by solvent-casting and the particulate-leaching method. Briefly, PCL–PEG–PCL was dissolved in chloroform at a concentration of 10% (w/v) and an n-CDAP slurry was added to produce composites with an n-CDAP content of 40 wt%. The mixture was stirred continuously for 2 hours and sodium chloride (NaCl) was added as a porogen (size: 400 μm; NaCl/PCL = 6/1, w/w), and the mixture was cast into Teflon molds containing 20 wells (well: $\Phi 12 \times 5$ mm). The samples were air-dried in a fume hood for 24 hours and subsequently vacuum-dried at 50°C for 48 hours to remove any remaining solvent. To leach out the salt, the dry samples were immersed in deionized water for 48 hours at room temperature, with water changes approximately every 12 hours. The scaffolds were dried in air for 24 hours and vacuum-dried overnight to obtain the resulting scaffolds. Using the same method, an n-HA–PCL–PEG–PCL composite scaffold was prepared as a control.

The phase composition of the n-CDAP–PCL–PEG–PCL composite was examined by X-ray diffraction (XRD; Geigerflex; Rigaku Co, Tokyo, Japan). The surface morphology of the composite scaffolds was examined by scanning electron microscopy (SEM; S-4300SE; Hitachi Ltd, Tokyo, Japan), and the porosity of the composite scaffolds was measured in distilled water by the Archimedes method. The average porosity was calculated based on five samples.

Degradability in vitro

The weight-loss ratio of n-CDAP–PCL–PEG–PCL and n-HA–PCL–PEG–PCL composite scaffolds sized

Φ12 × 5 mm during degradation in phosphate-buffered saline (PBS; pH 7.4) solution was measured using changes in dry weight after incubation for a specified time period. For such tests, the specimens were removed, rinsed in distilled water, and dried in a vacuum oven for 1 day. All the values presented are the average of three specimens. The percentage of weight loss was computed using the following equation:

$$\text{Weight loss} = 100\% \times W_0/W_t - W_0$$

where W_0 is the starting dry weight and W_t is the dry weight at time t.

Cell viability

Cell viability was evaluated after seeding MG-63 cells at a density of 5×10^4 cells on the n-CDAP–PCL–PEG–PCL and n-HA–PCL–PEG–PCL composite scaffolds with a size of Φ12 × 5 mm, followed by incubation for 1, 3, and 5 days, with the medium replaced every second day. Viable cells on substrates were assessed quantitatively using a MTT assay (MTT Kit; Roche Diagnosis Corp, Indianapolis, IN). In brief, cells/scaffold samples were placed in a culture medium containing MTT and incubated in a humidified atmosphere at 37°C for 4 hours. Cell growth was determined using a MTT assay. The absorbance value was measured at 570 nm using a microplate reader. Six specimens were tested at each incubation period, and each test was performed in triplicate. Results are reported as optical density (OD) units.

Alkaline phosphatase activity

To evaluate alkaline phosphate (ALP) activity, 5×10^4 MG-63 cells were seeded on the n-CDAP–PCL–PEG–PCL and n-HA–PCL–PEG–PCL composite scaffolds (tissue culture plate as a control) with a size of Φ12 × 5 mm. ALP activity was measured on days 1, 4, and 7. The adherent cells were removed from samples and lysed with PBS. A cell lysis buffer containing 0.1% Triton X-100 was added to the samples, which were then frozen. The frozen samples were thawed at 37°C for 5 minutes to measure the ALP activity according to the manufacturer's instructions (ALP kit 104; Sigma Aldrich, St Louis, MO). A 50 mL sample was mixed with 50 mL p-nitrophenol (1 mg/mL) in a 1 M diethanolamine buffer containing 0.5 mM $MgCl_2$ (pH 9.8) and incubated at 37°C for 15 minutes on a bench shaker. The reaction was stopped by adding 25 mL of 3 N NaOH per 100 mL of reaction mixture. The number of cells was determined by measuring the DNA content using Quant-iT™ Pico-Green dsDNA reagent kits (Molecular Probes, Eugene, OR). Sample DNA was quantified by measuring fluorescence with a Synergy HT Multi-Detection Microplate Reader (BioTek, Winooski, VT) at wavelengths of 480 nm excitation and 520 nm emissions. Enzyme activity was quantified by measuring absorbance at 405 nm, and ALP activity was calculated from a standard curve after normalizing the total DNA content.

Cell morphology

Samples with a size of Φ12 × 5 mm were used to evaluate MG-63 cells morphology cultured on the n-CDAP–PCL–PEG–PCL and n-HA–PCL–PEG–PCL composite. Approximately 50 mL of culture medium containing 5×10^4 cells was seeded on the top of the samples which had previously been placed in 24-well culture plates. Cells were allowed to attach to substrates for 4 hours, and then 1 mL of fresh culture medium was added to each well. Cells were incubated for 1, 3, and 5 days in a humidified atmosphere at 37°C and 5% CO_2. After the various culture times, sample cell constructs were washed twice with PBS solution and fixed with 4% formalin in PBS (pH 7.4) for 20 minutes. They were subsequently washed twice with PBS solution and dehydrated in a series of graded ethanol (50%, 60%, 70%, 80%, 90%, and 100% v/v) for 3 minutes each. Finally, specimens were air-dried in a desiccator overnight. Cell morphology on samples was observed under an S-4300SE FE-SEM (Hitachi).

Biocompatibility and osteogenesis in vivo

Biocompatibility and osteogenesis in vivo of the n-CDAP–PCL–PEG–PCL and n-HA–PCL–PEG–PCL composite scaffolds were evaluated using histological methods. Briefly, 12 healthy New Zealand white rabbits with an average weight of 3.0 kg were used for the implantation of the composite scaffolds. Under general anesthesia and sterile conditions, the left femur of each rabbit was exposed and one defect (Φ 6 mm) was drilled in the distal part of the femur. The bone cavities were washed to eliminate bone debris and dried with gauze. Cylindrical scaffolds with a size of Φ6 × 5 mm were implanted into the defects in the rabbit femora. Three animals from each group (one group as a control) were sacrificed by an abdominal overdose injection of pentobarbital sodium 1, 2, and 3 months after implantation. The samples together with surrounding tissue were excised, fixed in 10% neutral buffered formalin, decalcified, and embedded in paraffin. Tissue blocks were sectioned to 4 μm in thickness and stained with Masson's trichrome, and observed with light microscope (CX21; Olympus, Tokyo, Japan).

Statistical analysis

Statistical analysis was performed using one-way ANOVA with post hoc tests. All results are expressed as the mean ± standard deviation (SD). Differences were considered statistically significant at $P < 0.05$.

Results

TEM and XRD analysis

Figure 1 shows the morphology of the n-CDAP by TEM micrography. The synthetic n-CDAP was almost homogeneously rod-shaped and was around 20 nm in diameter and 80 nm in length. Figure 2 reveals the XRD pattern of the n-CDAP. The n-CDAP presented apatite phase with low crystallinity, and no additional phase was identified within detectable limits.

Characterization of composite scaffold

The n-CDAP–PCL–PEG–PCL composite scaffold is shown in Figure 3A. The surface morphology and microstructure of the composite scaffold with 40 wt% n-CDAP content under various magnifications are shown in Figure 3B and C. The composite scaffold exhibited a macroporous structure with completely open and interconnected pores. By SEM, the pores appeared almost irregular in shape, with diameters of around 400 μm as shown in Figure 3A. High-magnification SEM images further revealed that a number of small pores (around 10 μm) were distributed across the macroporous walls as shown in Figure 3B. The porosity of the composite scaffolds with 40 wt% n-CDAP prepared by this method was around 75%.

Examination at greater magnifications reveals that the composite scaffold surface exhibited typical spherical granules of apatite with the particles size of around 100 nm as shown in Figure 4. Most apatite particles were exposed on the composite surface except some n-CDAP granules, which were embedded in the PCL–PEG–PCL matrix.

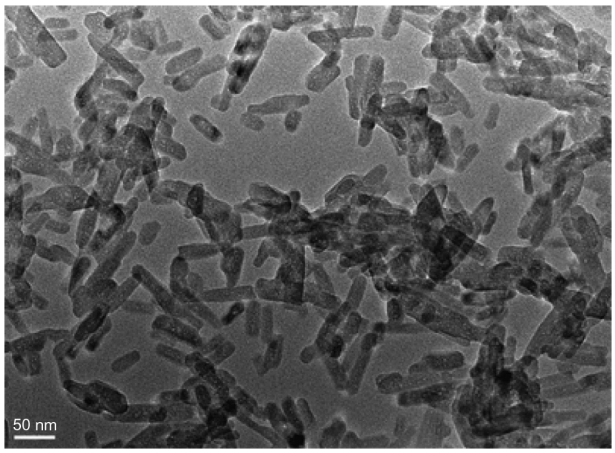

Figure 1 Transmission electron microscopy images of the morphology of nano calcium-deficient apatite.

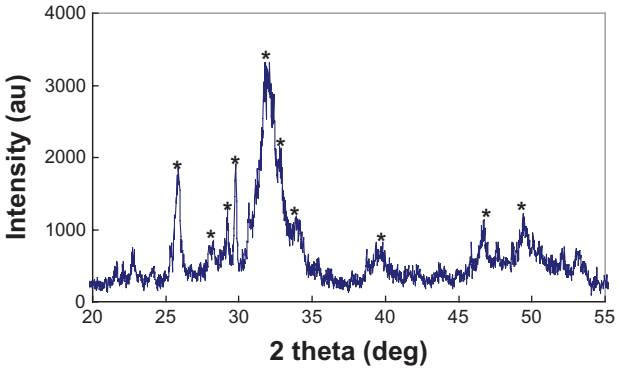

Figure 2 X-ray diffraction pattern of nano calcium-deficient apatite.
Note: *apatite peaks.

Degradation in vitro

Figure 5 presents the weight-loss ratio of n-CDAP–PCL–PEG–PCL composite scaffolds (with the n-HA–PCL–PEG–PCL composite scaffold as a control) as a function of incubation time in PBS. The weight loss in both types of samples increased with incubation time: 45 wt% and 35.2 wt% for both n-CDAP and n-HA composite scaffolds at 70 days, respectively. The weight-loss ratio for the n-CDAP composite scaffold was significantly greater than in the n-HA composite scaffolds during soaking in PBS for 70 days.

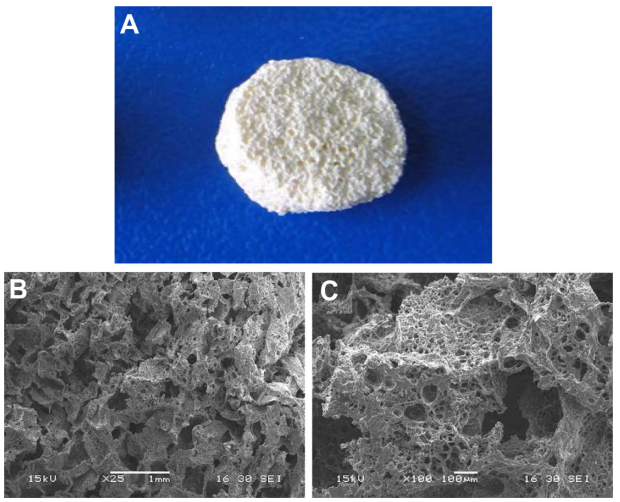

Figure 3 The n-CDAP–PCL–PEG–PCL composite scaffold (**A**), and scanning electron microscopy images of composite scaffold under different magnifications: (**B**) ×25 and (**C**) ×100.
Abbreviation: n-CDAP–PCL–PEG–PCL composite, nano calcium-deficient apatite and poly(ε-caprolactone)–poly(ethyleneglycol)–poly(ε-caprolactone).

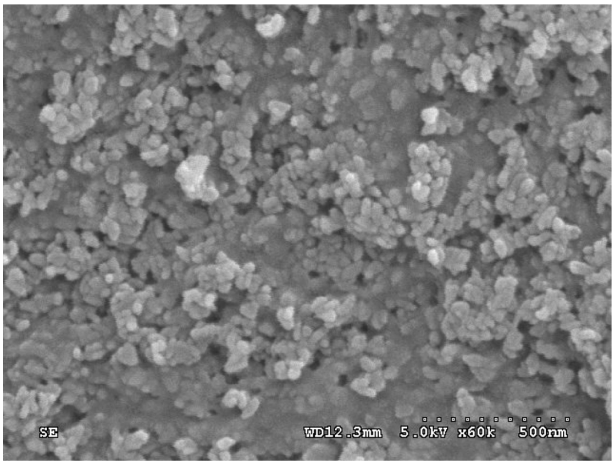

Figure 4 Scanning electron microscopy images of the n-CDAP–PCL–PEG–PCL composite scaffold surface.
Abbreviation: n-CDAP–PCL–PEG–PCL composite, nano calcium-deficient apatite and poly(ε-caprolactone)–poly(ethyleneglycol)–poly(ε-caprolactone).

Cell viability

The viability of MG-63 osteoblast-like cells cultured on n-CDAP–PCL–PEG–PCL composite scaffolds was assessed using the MTT assay, and n-HA–PCL–PEG–PCL composite scaffolds and tissue culture plate as controls. The optical density (OD) value for all the samples increased with time, and no significant differences were found for all the samples at 1 day (Figure 6). The OD values for the n-CDAP composite scaffold were significantly higher than in the n-HA composite scaffold at 3 and 5 days ($P < 0.05$). No significant differences appeared between composite and tissue culture plate (TCP) at 4 and 7 days. These results indicated that cell growth and viability (at 3 and 5 days) were superior in n-CDAP composite scaffolds than in n-HA composite scaffolds, suggesting that n-CDAP composite scaffolds facilitate cell growth and can promote cell viability.

Cell morphology

Figure 7 presents SEM micrographs showing the morphological features of MG-63 cells cultured on n-CDAP- and n-HA-based composite scaffolds at 3 days, respectively. At 3 days,

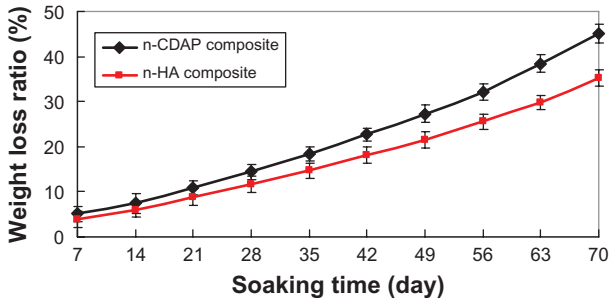

Figure 5 The weight-loss ratio of n-CDAP and n-HA composite scaffolds immersed in phosphate-buffered saline over time.
Abbreviations: n-CDAP, nano calcium-deficient apatite; n-HA, nano hydroxyapatite.

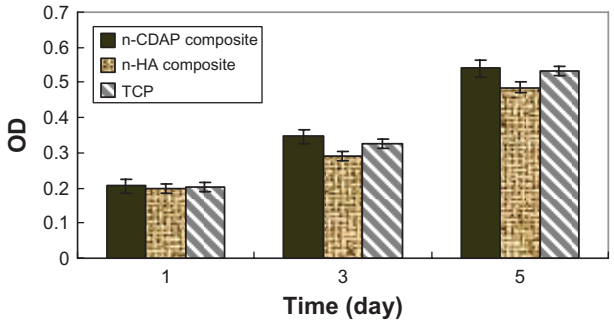

Figure 6 Viability of MG-63 cells on n-CDAP and n-HA composite scaffolds (with TCP as a control).
Abbreviations: n-CDAP, nano calcium-deficient apatite; n-HA , nano hydroxyapatite; TCP, tissue culture plate.

MG-63 cells had extended and spread well, and exhibited intimate contact with n-CDAP and n-HA composite surfaces. The results indicated that there are no significant differences in morphology of MG-63 cells cultured on the samples between n-CDAP- and n-HA-based composites, showing the cytocompatibility of both apatite composites.

Cell differentiation

ALP activity was assessed at 1, 4, and 7 days (Figure 8). At 1 and 4 days, ALP was expressed at lower levels, and no significant differences were detected among n-CDAP and n-HA composite scaffolds. Subsequently, ALP activity increased with time, and the cells on the n-CDAP and n-HA composites exhibited higher levels of ALP activity at 7 days than at 4 days, indicating that cells differentiated most at 7 days. Moreover, at 7 days, ALP activity on the n-CDAP composite was significantly greater than on the n-HA composite ($P < 0.05$).

Synchrotron radiation based microcomputed tomography analysis

X-ray microradiographic analysis confirms that the n-CDAP–PCL–PEG–PCL composite was biocompatible to the host bone and degradable in vivo. The n-CDAP composite scaffold materials appeared in the bone defect site at 1 month postimplantation, with a few bone tissue growths in the pores

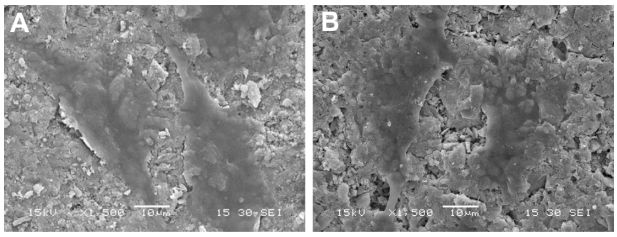

Figure 7 Scanning electron microscopy images of MG-63 cells cultured on n-CDAP (**A**) and n-HA (**B**) composite scaffolds for 3 days.
Abbreviations: n-CDAP, nano calcium-deficient apatite n-CDAPC; n-HA, nano hydroxyapatite.

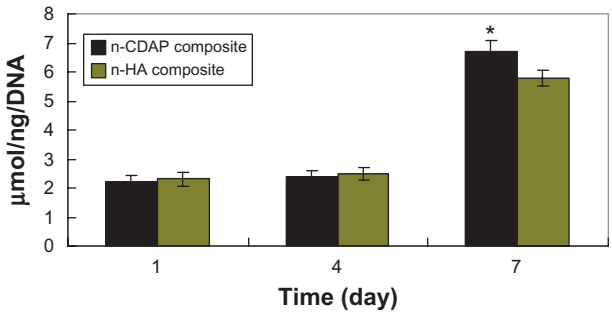

Figure 8 ALP activity of MG-63 cells cultured on n-CDAP and n-HA composite scaffolds over time.
Abbreviations: n-CDAP, nano calcium-deficient apatite; n-HA, nano hydroxyapatite; ALP, alkaline phosphate.

of the scaffold. The material–bone boundary became illegible at 2 months postimplantation, which suggests the increasing density of the implant, and partial composite degradation. The disappearance of the composite scaffold at 3 months after implantation indicated that the newly formed bone was formed in the bone defect site, which was similar to the host bone; showing most of the materials were degradable and substituted by new bone.

Histological evaluation

At 1 month postoperation, a few newly formed bone tissues were found deposited at the interface between the composite scaffold materials and host bone tissue with the presence of active osteoblasts (Figure 10A and B). At 2 months postoperation, more newly formed bone tissues were found deposited at the interface between the composite scaffold materials

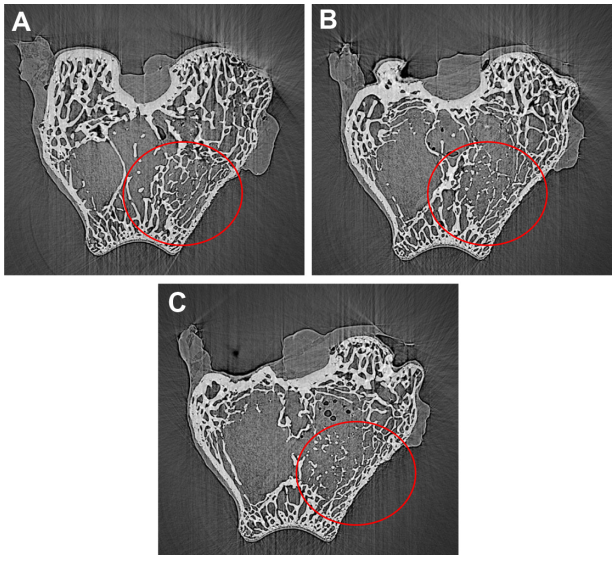

Figure 9 SR m-CT of cross-section images of n-CDAP–PCL–PEG–PCL composite scaffolds implanted into bone defects of rabbit femora for (**A**) 1, (**B**) 2, and (**C**) 3 months.
Abbreviation: n-CDAP-PCL–PEG–PCL, nano calcium-deficient apatite and poly (ε-caprolactone)–poly(ethyleneglycol)–poly(ε-caprolactone).

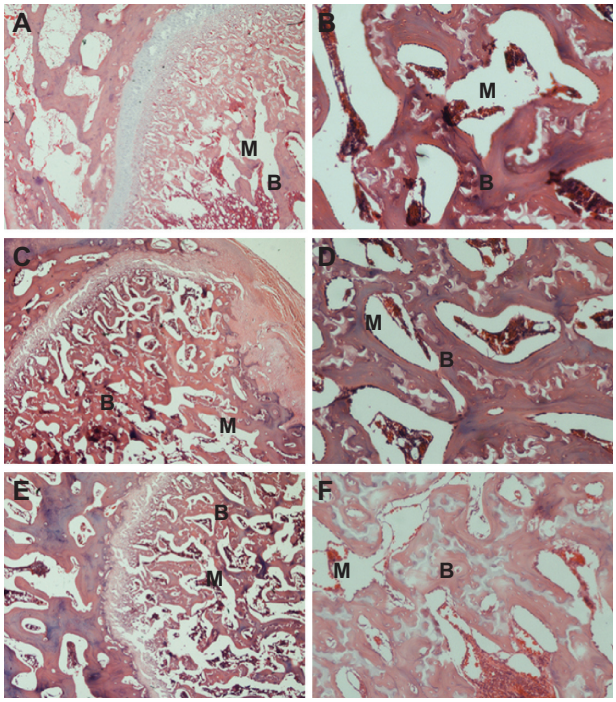

Figure 10 Hematoxylin and eosin-stained section of n-CDAP/PCL–PEG–PCL composite scaffolds implanted into bone defects of rabbit femora for (**A** and **B**) 1, (**C** and **D**) 2, and (**E** and **F**) 3 months. M represents gradually degraded materials and B represents new bone tissue, respectively.
Abbreviation: n-CDAP-PCL–PEG–PCL, nano calcium-deficient apatite and poly (ε-caprolactone)–poly(ethyleneglycol)–poly(ε-caprolactone).

and host bone tissue, and the amount of bone matrix on the composite scaffolds was observed (Figure 10C and D). At 3 months, new bone regenerated and penetrated through the interconnected pores into the center of the composite scaffolds (Figure 10E and F). The boundary between scaffold material and host bone was unclear due to the amount of mature bone tissue that grew into the pores of the composite scaffold.

Figure 11 shows the area of new bone formation within bone defects after n-CDAP and n-HA composite scaffolds were implanted in vivo for 1, 2, and 3 months. New bone

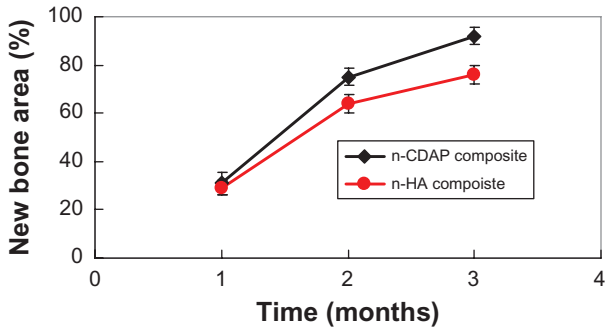

Figure 11 New bone tissue area in bone defects after n-CDAP and n-HA composite scaffolds implanted in vivo for 1, 2, and 3 months.
Abbreviations: n-CDAP, nano calcium-deficient apatite; n-HA, nano hydroxyapatite.

area significantly increased for both n-CDAP and n-HA composites after being implanted into bone defects for 1, 2, and 3 months. No obvious difference for new bone area was found between n-CDAP and n-HA composites at 1 month. However, the new bone area for n-CDAP was significantly higher than for the n-HA composite at both 2 and 3 months ($P < 0.05$).

Discussion

In recent years, considerable efforts have been spent on research and development of biocomposites for bone defect repair, and some studies have shown that bioactive and biodegradable organic/inorganic composites could play important roles in bone regeneration.[15,16] A biocompatible and biodegradable porous scaffold is a temporary scaffold, which is gradually degradable with new bone tissue regeneration in bone defects after scaffold implanted in vivo.[17] A study has shown that a deficient calcium apatite called nonstoichiometric apatite with a Ca/P of 1.50 was biologically more active than pure bioactive apatite ceramics alone because it has a composition and structure very close to natural bone minerals.[12]

In this study, n-CDAP–PCL–PEG–PCL bioactive and biodegradable composite scaffolds with 40 wt% n-CDAP content were fabricated, and the composite scaffolds exhibited a homogeneous distribution of open macropores and pore sizes around 400 μm, and scaffolds had a good degree of interconnectivity pores. Therefore, the characteristic of the composite scaffolds is likely beneficial for facilitating cell growth. Some micropores with diameters of around 10 μm were dispersed on the macroporous walls of the n-CDAP–PCL–PEG–PCL composite scaffolds, which might have been introduced during evaporation of the solvent. These micropores might play important roles in nutrient diffusion and improve the degradability of the composite scaffolds. Yuan et al reported that micropores on the macroporous walls of a calcium phosphate ceramic were important in osteoinduction, and could induce new bone formation in the scaffolds.[18] Therefore, micropores on the macroporous surface may help enhance the biological performance of the composite scaffolds.

Proper degradation of implanted materials in the physiological environment is one of the most important characteristics of the scaffold for usefulness in bone tissue engineering.[19] The fabricated n-CDAP–PCL–PEG–PCL and n-HA–PCL–PEG–PCL composite scaffolds exhibited weight loss in PBS over time, which indicates their degradability in vitro. Essentially all of the weight lost from the composite scaffold was due to the degradation (dissolution) of both the nanoapatite and PCL–PEG–PCL. In addition, the weight-loss ratio of the n-CDAP–PCL–PEG–PCL was significantly greater than n-HA–PCL–PEG–PCL composite scaffolds after soaking for 70 days. Therefore, if the two composite scaffolds were to be implanted into the body, the composites would gradually degrade in vivo, and n-CDAP-based composites would degrade faster than n-HA-based composites.

Bioactive biomaterials need to interact actively with cells and stimulate cell growth.[20] The MG-63 osteoblast-like cells were viable on both n-CDAP- and n-HA-based composite scaffolds, as demonstrated by the MTT assay. Both n-CDAP and n-HA composites could stimulate MG-63 cell growth and viability over time. The nanoapatite exposed on the composite surfaces may have additional special surface properties that promote cell viability. The composite surface features of n-CDAP and n-HA particles may be responsible for stimulating cell growth and viability. Cell viability on the n-CDAP composites was significantly higher than on n-HA-based composites, which indicates that n-CDAP had special properties for cell growth. The dissolution of n-CDAP was bigger than n-HA, which might release more Ca^{2+} from the apatite and affect cell behaviors.[12] The superior viability of MG-63 cells on the n-CDAP–PCL–PEG–PCL composite is probably associated with differing material surface features between the n-CDAP and n-HA composite scaffolds.

ALP activity has been used as an early marker for functionality and differentiation of osteoblasts during in vitro experiments.[21] In this study, ALP activity on the n-CDAP–PCL–PEG–PCL composite scaffolds exhibited significantly higher levels of expression than those of n-HA–PCL–PEG–PCL composite scaffolds at 7 days, indicating that cells differentiated more quickly after being cultured on the n-CDAP- than n-HA-based composites. Therefore, the most distinct advantage of the n-CDAP-based composite scaffolds appears to be the superior effect on ALP activity compared to n-HA-based composite scaffolds. This increased activity probably resulted from the surface features for the n-CDAP-based composite scaffolds as compared with n-HA-based composite scaffolds, which might be responsible for stimulating cell differentiation.

The in vitro experiment results prompted us to investigate the bioproperties of both the n-CDAP–PCL–PEG–PCL and n-HA–PCL–PEG–PCL composite scaffolds in vivo. A rabbit model (bone defect) was used to investigate the hard tissue response to the composite scaffold in this study. To monitor the process of the formation of bone tissue, SR m-CT and histological studies were performed on the composite specimens after different implantation periods. Active bone

regeneration in the rabbit bone defects was found in the composite scaffolds, which shows that the porous composite scaffold enhanced bone regeneration efficiency.

The degradation of the implanted biocompatible materials has been addressed in many studies, and chemical dissolution and cell-mediated resorption have been suggested for these biomaterials.[22] In this study, the degradation of the n-CDAP–PCL–PEG–PCL composite scaffolds was observed after implantation in the defects of the rabbits for 1, 2, and 3 months. As the implantation time prolonged, new bone regenerated and gradually penetrated into the scaffolds accompanied by the resorption of the composite scaffold materials. The results showed that n-CDAP–PCL–PEG–PCL composite scaffolds had good biocompatibility, biodegradability, and osteogenesis.

The area of newly formed bone gradually increased with time, which indicates that new bone tissue gradually regenerated within bone defects after n-CDAP–PCL–PEG–PCL composite scaffolds were implanted in vivo. Seventy-five percent and 92% of the bone defect area were filled with new bone tissue after n-CDAP-based composites were implanted for 2 and 3 months, respectively. However, the area of new bone was 64% and 76% after n-HA-based composite scaffolds were implanted for 2 and 3 months, respectively. The results suggest that the n-CDAP-based composite scaffolds exhibited higher efficiency of bone regeneration compared with n-HA-based composite scaffolds because the n-CDAP-based composite scaffolds had better bioactivity and biodegradability than n-HA-based composite scaffolds. In conclusion, the n-CDAP-based composite scaffolds improved its bioperformance by addition into PCL–PEG–PCL, and showed faster and more effective osteogenesis compared with n-HA-based composite scaffolds.

Conclusion

Biocomposite scaffolds of n-CDAP and PCL–PEG–PCL were synthesized using a solvent-casting and particulate-leaching method, which had a porosity of around 75% with open and interconnected pores around 400 μm. The degradation ratio of the n-CDAP–PCL–PEG–PCL composite scaffolds was faster than n-HA–PCL–PEG–PCL composite scaffolds during soaking in PBS for 70 days. The viability ratio of MG-63 cells was significantly higher in the n-CDAP–PCL–PEG–PCL composite scaffolds than in n-HA–PCL–PEG–PCL composite scaffolds with an apatite content of 40 wt% at 3 and 5 days, which demonstrates that the n-CDAP–PCL–PEG–PCL composite could stimulate cell viability. Furthermore, the level of ALP activity was obviously higher in the n-CDAP–PCL–PEG–PCL than in the n-HA–PCL–PEG–PCL composite scaffolds at 7 days, which shows that the n-CDAP composite promotes cell differentiation. The n-CDAP–PCL–PEG–PCL biocomposite had excellent in vitro biocompatibility and bioactivity. Histological evaluation results confirmed that composite implants exhibited high efficiency in bone regeneration.

Acknowledgments

This study was supported by grants from the Major Program of Natural Science Foundation of Shanghai, China (No 11JC1416302).

Disclosure

The authors report no conflicts of interest in this work.

References

1. Zhou H, Lee J. Nanoscale hydroxyapatite particles for bone tissue engineering. *Acta Biomater*. 2011;7(7):2769–2781.
2. Zhang CY, Lu H, Zhuang Z, et al. Nano-hydroxyapatite/poly (L-lactic acid) composite synthesized by a modified in situ precipitation: preparation and properties. *J Mater Sci Mater Med*. 2010;21(12): 3077–3083.
3. Huang D, Zuo Y, Zou Q, et al. Antibacterial chitosan coating on nano-hydroxyapatite/polyamide66 porous bone scaffold for drug delivery. *J Biomater Sci Polym E*. 2011;22(7):931–944.
4. Dorozhkin SV. Nanosized and nanocrystalline calcium orthophosphates. *Acta Biomater*. 2010;6(3):715–734.
5. Ngiam M, Liao SS, Patil AJ, et al. The fabrication of nano-hydroxyapatite on PLGA and PLGA/collagen nanofibrous composite scaffolds and their effects in osteoblastic behavior for bone tissue engineering. *Bone*. 2009;45(1):4–16.
6. Cui Y, Liu Y, Cui Y, et al. The nanocomposite scaffold of poly (lactide-co-glycolide) and hydroxyapatite surface-grafted with L-lactic acid oligomer for bone repair. *Acta Biomater*. 2009;5(7):2680–2692.
7. Lao LH, Wang YJ, Zhu Y, et al. Poly(lactide-co-glycolide)/hydroxyapatite nanofibrous scaffolds fabricated by electrospinning for bone tissue engineering. *J Mater Sci Mater Med*. 2010;22(8):4374–4378.
8. Ma GL, Miao BL, Song CX. Thermosensitive PCL-PEG-PCL Hydrogels: Synthesis, Characterization, and Delivery of Proteins. *J Appl Polym Sci*. 2010;116(4):1985–1993.
9. Gou ML, Zheng L, Peng XY, et al. Poly(epsilon-caprolactone)-poly(ethylene glycol)-poly(epsilon-caprolactone) (PCL-PEG-PCL) nanoparticles for honokiol delivery in vitro. *Int J Pharm*. 2009;375(1–2): 170–176.
10. Gou ML, Gong CY, Zhang J, et al. Polymeric matrix for drug delivery: Honokiol-loaded PCL-PEG-PCL nanoparticles in PEG-PCL-PEG thermosensitive hydrogel. *J Biomed Mater Res A*. 2010;93(1): 219–226.
11. Mochales C, Wilson RM, Dowker SEP, et al. Dry mechanosynthesis of nanocrystalline calcium deficient hydroxyapatite: Structural characterization. *J Alloys Compd*. 2011;509(27):7389–7394.
12. Sponer P, Strnadova M, Urban K et al. In vivo behaviour of low-temperature calcium-deficient hydroxyapatite: comparison with deproteinised bovine bone. *Int Orthop*. 2011;35(10):1553–1560.
13. Otsuka M, Hirano R. Bone cell activity responsive drug release from biodegradable apatite/collagen nano-composite cements-In vitro dissolution medium responsive vitamin K2 release. *Colloids Surf B Biointerfaces*. 2011;85(2):338–342.

14. Nichols HL, Zhang N, Zhang J, et al. Coating nanothickness degradable films on nanocrystalline hydroxyapatite particles to improve the bonding strength between nanohydroxyapatite and degradable polymer matrix. *J Biomed Mater Res A*. 2007;82(2):373–382.
15. Sun F, Zhou H, Lee J. Various preparation methods of highly porous hydroxyapatite/polymer nanoscale biocomposites for bone regeneration. *Acta Biomater*. 2011;7(11):3813–3828.
16. Marelli B, Ghezzi CE, Mohn D. Accelerated mineralization of dense collagen-nano bioactive glass hybrid gels increases scaffold stiffness and regulates osteoblastic function. *Biomaterials*. 2011;32(34):8915–8926.
17. Chen L, Tang CY, Chen DZ. Fabrication and characterization of poly-D-L- lactide/nano-hydroxyapatite composite scaffolds with poly (ethylene glycol) coating and dexamethasone releasing. *Compos Sci Technol*. 2011;71(16):1842–1849.
18. Yuan HP, Kurashina K, de Bruijn JD. A preliminary study on osteoinduction of two kinds of calcium phosphate ceramics. *Biomaterials*. 1999;20(19):1799–1806.
19. Wei L, Cai CH, Lin JP, et al. Degradation controllable biomaterials constructed from lysozyme-loaded Ca-alginate microparticle/chitosan composites. *Polymer*. 2011;52(22):5139–5148.
20. Hertz A, Bruce IJ. Inorganic materials for bone repair or replacement applications. *Nanomedicine*. 2007;2(6):899–918.
21. Zhao CL, Cao P, Ji WP, et al. Hierarchical titanium surface textures affect osteoblastic functions *J Biomed Mater Res A*. 2011;99(4):666–675.
22. Bashoor-Zadeh M, Baroud G, Bohner M. Simulation of the in vivo resorption rate of beta-tricalcium phosphate bone graft substitutes implanted in a sheep model. *Biomaterials*. 2011;32(27):6362–6373.